Journal of Alloys and Compounds 748 (2018) 163–170

Contents lists available at ScienceDirect

Journal of Alloys and Compounds

journal homepage: http://www.elsevier.com/locate/jalcom

Nanotwins induced by pulsed laser and their hardening effect in a Zr alloy

Linjiang Chai [a, *], Ke Chen [a], Yan Zhi [a], Korukonda L. Murty [b], Liang-Yu Chen [c, **], Zhinan Yang [d]

[a] College of Materials Science and Engineering, Chongqing University of Technology, Chongqing, 400054, China
[b] Department of Nuclear Engineering, North Carolina State University, Raleigh, NC 27695-7909, USA
[c] School of Science, Jiangsu University of Science and Technology, Zhenjiang, Jiangsu 212003, China
[d] National Engineering Research Center for Equipment and Technology of Cold Strip Rolling, Yanshan University, Qinhuangdao, 066004, China

ARTICLE INFO

Article history:
Received 6 December 2017
Received in revised form
19 February 2018
Accepted 10 March 2018
Available online 13 March 2018

Keywords:
Zr alloy
Pulsed laser
Nanotwins
Hardening
Electron backscatter diffraction

ABSTRACT

A pulsed laser was employed to treat a Zr-2.5Nb alloy with laser-induced microstructures (especially dense nanotwins) characterized by electron channeling contrast imaging (ECC) imaging and electron backscatter diffraction (EBSD) techniques. Hardening effect of the nanotwins was derived by analyzing hardness contributions from various microstructural factors modified by the pulsed laser treatments (PLT). Results show that dense nanotwins, that are difficult to introduce into Zr alloys by conventional thermo-mechanical methods, can be readily produced by the PLT at laser powers of 50 and 100 W. The twinning system is determined to be the compressive type of {10−11}⟨10−12⟩ by orientation analyses using EBSD. After the PLT, specimen hardness is markedly increased, which could be attributed to not only grain refinement and solid solution of Nb but more considerably to the abundance of the {10−11} nanotwins, demonstrating their strong hardening effect.

1. Introduction

In recent years, nanotwins have received wide and ever-increasing interests from both academia and industries because of their demonstrated superiority in enhancing mechanical properties of structural metallic materials [1,2]. To obtain high density of nanotwins, various materials processing techniques have been attempted by different research groups with effective methods including electro-deposition, dynamic plastic deformation, surface mechanical attrition treatment, etc [3]. It is to be noted that such attractive nanotwins have to-date been mainly found and studied in metals with a cubic structure such as Cu and austenitic stainless steel [4,5]. Most methods working well for introducing nanotwins into cubic metals are found to be less effective after applying to hexagonal-close-packed (hcp) metals [1]. As a consequence, dense twins have relatively rarely been observed in nanostructured hcp materials although twinning is well-known to play a crucial role in deforming their coarse-grained counterparts [6].

Zr alloys with hcp α phase at room temperature have important structural applications in chemical and nuclear industries owing to excellent corrosion resistance and nuclear properties [7–10]. Earlier studies revealed that extensive twinning activities can be observed in α-Zr deformed under specific conditions (favorable initial texture [11–13], low temperature [12,14,15], high strain rate [13,15–17], large grain [15,18], etc). However, twins in all these reports are found to have (sub-) microscale thicknesses, much thicker than that of desirable nanotwins. In contrast with the difficulty of producing dense nanotwins in α-Zr through conventional thermo-mechanical processing, our recent work showed that they could be obtained in a commercially pure Zr with pulsed laser surface treatments [19]. More attentions should be received by the pulsed laser-induced nanotwins to better reveal their specific characteristics and effects on properties.

In the present work, a Zr-2.5Nb alloy was subjected to the pulsed laser treatments (PLT) at two different powers, with microstructures containing abundant nanotwins expected to be produced. Detailed microstructural characterization for the nanotwins was then performed by electron channeling contrast (ECC) imaging and electron backscatter diffraction (EBSD) techniques. Based on the experimental results, origin and hardening effect of the PLT-

* Corresponding author.
** Corresponding author.
E-mail addresses: chailinjiang@cqut.edu.cn (L. Chai), lychen@just.edu.cn (L.-Y. Chen).

https://doi.org/10.1016/j.jallcom.2018.03.126
0925-8388/

induced nanotwins were analyzed and discussed.

2. Experimental

An as-received hot-deformed (forged to a strain of ~30%) Zr-2.5 wt% Nb alloy was selected as the starting material, with its melting point estimated as ~1800 °C. Rectangular specimens with the dimension of 3 mm × 8 mm × 15 mm along thickness, width and length directions (denoted as TD, WD and LD, respectively) were cut from the as-received Zr alloy material. LD-WD surfaces of the as-cut specimens were chemically cleaned using a mixed solution of 10 vol% hydrofluoric acid, 45 vol% nitric acid and 45 vol% distilled water and then subjected to pulsed laser irradiation (with the beam parallel to the TD) by use of a pulsed 600W Nd: YAG laser device. During the PLT, the irradiated areas were protected by continuously blown Ar gas to prevent oxidation. Two laser powers (50 and 100 W) were used in this work, with corresponding power densities of 63.7 and 127.4 W/mm^2, and energy densities of 6.3 and 12.5 J/mm, respectively. Other treatment parameters were kept the same: pulse duration 5 ms, pulse frequency 20 Hz, beam diameter 1 mm, defocusing amount +2 mm and beam travel speed 8 mm/s along the LD (throughout the specimen length).

A Zeiss Sigma HD field emission gun scanning electron microscope (FEGSEM) was used to investigate microstructural characteristics induced by the laser surface treatment. For direct microstructural observation, ECC images of backscattered electrons were taken, with demonstrated ability to reveal various crystallographic orientation-related defects like nanotwins [19–21]. For quantitative orientation analyses, on the other hand, an EBSD system with a NordlysMax^2 detector attached to the FEGSEM was utilized. Both the ECC and the EBSD examinations were performed on TD-WD surfaces (normal to the travel direction of the laser beam) of the specimens, with their preparation procedures already detailed elsewhere [22]. Hardness measurements were also made using a Vickers indentation tester (HVS-1000) for the as-received and the laser-treated specimens, with indentations located near the beam center in the latter ones (on the LD-WD surfaces). At least ten measurements were carried out for each specimen to calculate an average value. For each measurement, the applied load was 0.98 N (100 g) with a dwell time of 10 s.

3. Results

3.1. Microstructural characteristics

An ECC image of the as-received material is shown in Fig. 1a, from which a dual-phase microstructure consisting of bulk α grains and thin β films can be seen. The co-existence of α-Zr and β-Zr is also confirmed after performing EBSD indexing for both of them, as shown in Fig. 1b. For the α phase, varied contrasts in Fig. 1a suggest differences in their grain orientations due to the electron channeling effect [20]. On the other hand, the β films (~10% in volume fraction) are found to be always brighter compared to the α grains, which should be related to atomic number (Z) contrast of the backscattered electrons. Such a contrast effect enables a high-Z element to appear lighter than a low-Z element [23]. With respect to the case of Zr-Nb alloys, the atomic number of Nb ($Z_{Nb} = 41$) is slightly higher than that of Zr ($Z_{Zr} = 40$). It is thus known than the β phase is more Nb-enriched than the α phase in the as-received Zr-2.5Nb material, consistent with earlier reports [8,24]. In regards to phase dimensions, grain sizes of the α phase are found to spread from submicron to near ten micrometers while the β-film thicknesses limited to a few hundred nanometers. Average values of the α-grain size and the β-film thickness are measured to be about 1.4 μm and 72 nm, respectively. More specific orientation characteristics corresponding to the starting microstructure have been documented in our recent work [25].

Cross-sectional microstructures of the two PLTed specimens are presented in Fig. 2. Melting zones (MZs) of both the specimens are marked in Fig. 2a and b (low-magnification images). The maximum MZ widths of the 50 W and the 100 W specimens are measured to be about 850 and 1000 μm, respectively, with corresponding depths of 150 and 230 μm. This means that an increase of laser power is able to produce enlarged molten pools during laser irradiation. Closer observations (Fig. 2c and d) reveal that the MZs in both the laser-treated specimens are completely comprised of α-plate structures without any residual β phase. Most of these α plates are found to have submicron widths and their average value is determined by the linear intercept method to be about 290 nm in both the specimens. Clearly, remarkable α-grain refinements are induced by the PLT, compared to the starting microstructure. Additionally, after further magnified observations for the plate structures, a large number of small twins are found to extensively exist inside these plates (Fig. 2e and f). Measurements for such twins show that they essentially have lamellar thicknesses below a hundred nanometers, with the majority ranging from 30 to 70 nm. No evident difference is detected for sizes of the nanotwins in the specimens laser-treated at different powers. Nevertheless, their density seems to be slightly higher in the 100 W specimen. In consideration of the ultrafast cooling that can be induced by the PLT, the microstructures in the MZs are believed to correspond to twinned martensites. Also, the absence of β phase suggests

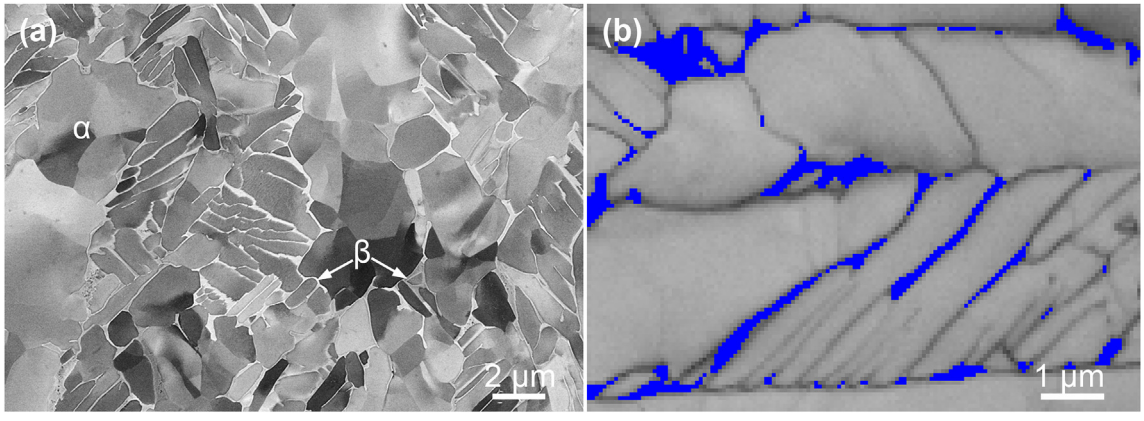

Fig. 1. The starting microstructure of the Zr-2.5Nb alloy: (a) ECC image and (b) EBSD band contrast map (step size 60 nm); the indexed β-Zr is colored blue in (b). (For interpretation of the references to color in this figure legend, the reader is referred to the Web version of this article.)